

In situ ESR Observation of Interface Dangling Bond Formation Processes During Ultrathin SiO₂ Growth On Si(111)

W. Futako,¹ N. Mizuochi,^{1,2} and S. Yamasaki¹

¹*Diamond Research Center, AIST Tsukuba Central, 1-1-1 Umezono, Tsukuba, Japan 305-8568*

²*Institute of Library and Information Science, University of Tsukuba, 1-2 Kasuga, Tsukuba, Japan 305-8550*

(Received 4 August 2003; published 12 March 2004)

We report the formation processes of interface dangling bonds (P_b centers) during initial oxidation of a clean Si(111) surface using an ultrahigh-vacuum electron-spin-resonance technique. At the oxidation of one or two Si layer(s), the P_b center density reached around $2.5\text{--}3.0 \times 10^{12} \text{ cm}^{-2}$, which is the same density as in the case of thick SiO₂. This result shows that the P_b center density does not originate from the long-range accumulation of the structural stress between two materials, but from the chemical reactions of oxidation within a few Si atomic layers.

DOI: 10.1103/PhysRevLett.92.105505

PACS numbers: 61.72.Hh, 68.55.Ln, 73.20.-r, 76.30.-v

Silicon oxidation is not only one of the key processes of Si large-scale-integration engineering but also a major subject in physics through the research of its reaction mechanism and defect properties. As a typical point defect at the Si/SiO₂ interface affecting electrical properties, a threefold coordinated silicon atom with a neutral charge, the so-called P_b center, has been widely investigated [1–7]. Electron spin resonance (ESR) is one of the most powerful tools available for investigating P_b centers. There have been many reports on the use of ESR for characterizing the atomic structure of P_b centers [1,6,7], electric level [3–6], typical density and its dependence on the oxidation temperature [2–4], etc. However, these studies have been limited to the static structure of Si/SiO₂ after Si oxidation, whereas microscopic information about the dynamic oxidation mechanism is required. Also, from an engineering point of view, understanding of the nature of thin SiO₂ is important even as the interfacial layer with high- k (dielectric constant) materials intensively investigated for a recent couple of years [[8,9] and reference therein].

Previously, we have developed an ultrahigh-vacuum (UHV)-ESR system, which is a combination of an ESR system and a UHV chamber, and reported the dynamic oxygen [10] and hydrogen [11] termination processes on a Si(111)- 7×7 surface, we observed the appearance and dynamic change of the adatom dangling bond (DB) signal at room temperature [10]. Regarding SiO₂ formation, however, since Si oxidation does not proceed deeply at room temperature, the detailed processes of formation of SiO₂ were not obtained. In this study, we focused on the process of P_b center generation during subsequent silicon oxidation after oxygen termination on a clean Si(111) surface at high temperatures, and succeeded in observing the dynamic process of formation of P_b centers, based on which we discuss the microscopic origin of P_b centers.

A continuous wave (cw) X-band (≈ 9.5 GHz) ESR spectrometer (Bruker E-500) was attached to a UHV chamber with a sample cell made of a silica tube (diameter = 10 mm) [10]. The UHV chamber was arranged so that the sample cell was located within a microwave cavity of an ESR system. The base pressure of the UHV chamber was less than 10^{-10} Torr. Si(111) wafers were used as samples. The resistivity of the silicon substrate was higher than 2000 Ω cm. The sample area for ESR measurements was $10 \times 3 \text{ mm}^2$ with both sides polished. Samples were cleaned by the conventional chemical treatment, RCA cleaning [12], before being set in the chamber. The sample was supported at the end of a vacuum transfer rod. This setup enabled precise background subtraction, resulting in a high signal-to-noise ratio, since the position of the silica tube and the sample in the microwave ESR cavity determining the baseline fluctuation is highly reproducible over a series of measurements. Before ESR measurements, samples were preheated to 900 K in the UHV chamber for degassing. The transfer rod rotates in the (1 $\bar{1}$ 0) plane so that the ESR spectrum can be measured as a function of the angle, θ , between the [111] direction of the Si substrate and the magnetic field \mathbf{B} [10]. Typical microwave power, modulation frequency, and modulation amplitude in the present study were 0.6 mW, 100 KHz, and 1 G, respectively. Spin densities were determined relative to a CuSO₄(H₂O)₅ intensity standard. The g value of the sample was calibrated relative to a diphenylpicrylhydrazyl (DPPH: $g = 2.0036$) standard sample.

The Si(111)- 7×7 clean surface was prepared by direct-current heating of the wafer at 1570 K followed by slow cooling. The 7×7 surface structure was confirmed using reflection high-energy electron diffraction (RHEED). Oxidation was carried out around 1050 K. Oxygen dose, to which the clean silicon surface was exposed, was controlled by the pressure (1×10^{-6} – 8×10^{-3} Torr) and the exposure time. Generally, since the

interface defect density is severely affected by impurities such as H_2O or H atoms in the system [2,13], it is very difficult to obtain its true number. In addition to use of the UHV experimental condition, in order to avoid generation of hydrogen atoms terminating P_b centers, we took care that the ionization gauges were located far from the sample position and almost turned off during experiments. These efforts enable us to detect the interface defect so stably during ESR measurements without hydrogen termination effects.

Auger electron (AE) spectroscopy was used to estimate the SiO_2 thickness on the silicon substrate [14]. A measured AE spectrum for a SiO_2/Si sample was simulated by a linear combination of the Si and SiO_2 (> 5 nm) reference spectra with the SiO_2 thickness varied as the fitting parameter. The escape depth of the Auger electrons was assumed to be 0.6 nm for both Si and SiO_2 . Although there is some ambiguity as to SiO_2 thickness depending on the difference between Si(100) [14] and present study of Si(111), it does not affect the conclusion in the present study. All measurements (ESR, RHEED, and AES) were carried out at room temperature.

Figure 1 shows ESR spectra of a Si(111) sample after chemical cleaning, and before and after thermal oxidation, where $\theta = 0^\circ$ (the direction of magnetic field was parallel to the [111] axis of the Si substrate). The interface defect density and the peak-to-peak linewidth (ΔB_{p-p}) of chemical oxide [(1) in Fig. 1] is $4.2 \times 10^{12} \text{ cm}^{-2}$ and 2.1 G, respectively. These values are consistent with the

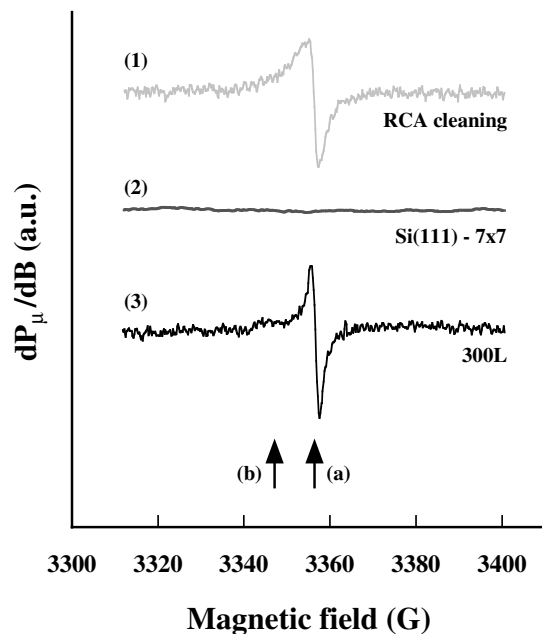


FIG. 1. ESR spectra (1) after wet cleaning, (2) of Si(111) – 7×7 surface after thermal annealing at 1570 K, and (3) after thermal oxidation with 300 L exposure at 1050 K. (a) and (b) indicate the positions of magnetic field of a P_b center [2,6] and of a shoulder structure (details are described in the text), respectively.

105505-2

typical P_b center [2,4,6]. As shown in Fig. 1(2), the Si(111)- 7×7 clean surface shows no significant signal indicating that the DB at the interface with chemical oxide disappears. However, it should be noted that the 7×7 structure should have a large density of DBs despite the lack of ESR signal. This contradiction can be explained as the delocalizing effect of DB wave functions caused by the metallic nature of the Si(111)- 7×7 surface structure, as described in detail elsewhere [10].

At 1050 K, introduction of oxygen molecules of approximately 300 L ($1 \text{ L} = 1 \times 10^{-6} \text{ Torr s}$) resulted in the appearance of ESR signals as shown in Fig. 1(3). An AE spectrum of this condition showed a SiO_2 pattern, indicating that an oxide layer had already grown. In the previous study at room temperature [10], we observed two dynamic changes: (i) oxygen-atom termination process of Si clean surface, and (ii) oxygen-atom covering on adatom DBs. In this study, the subsequent SiO_2 formation processes are immediately started because of the high-temperature oxidation, where a high oxidation rate readily completes the processes of (i) and (ii) even for a small amount of oxygen dose [14].

The ΔB_{p-p} and the g value of the main signal (a) after the thermal oxidation are 2.0 G and 2.0013 for $\theta = 0^\circ$, respectively, independent of oxidation thickness under the present conditions. The slightly smaller ΔB_{p-p} and the different line shape compared to that of chemical oxide [Fig. 1(1)] are consistent with the literature [2]. The angular dependence of g value against the magnetic field is plotted in Fig. 2. The gray line indicates the g map known for the P_b center whose principal values in the g matrix are $g_{zz} = g_{\parallel} = 2.0014$ and $g_{xx} = g_{yy} = g_{\perp} = 2.0086$ [2,6]. This experimental result shown in Fig. 2 confirmed that the ESR signals observed here originate from P_b centers.

As indicated by (b) in Fig. 1, a shoulder structure in the lower magnetic field was observed. The signal approximately doubled for a silicon substrate of twice the thickness. This suggests that the shoulder structure originates from DBs grown on the side surface of the $(\bar{1}\bar{1}2)$ plane. In

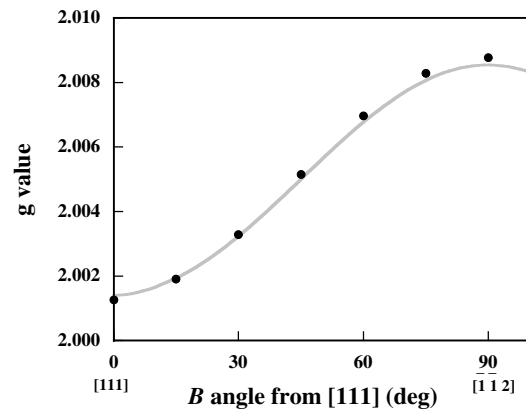


FIG. 2. The g map for the observed signal. The solid curve indicates the known g map for the P_b center [2,6].

105505-2

the subsequent sections, we focus only on the main signal from the [111] P_b center by carefully subtracting the shoulder structure from the entire spectra.

In Fig. 3, the effective spin density of the main signal is plotted as a function of the oxygen dose. The P_b density after wet chemical cleaning is also shown for comparison. SiO_2 thickness indicated in the figure is estimated by AE spectroscopy (< 1.1 nm) and by ellipsometry (> 6 nm). All samples are oxidized at 1050 K except for the wet cleaned sample.

For O_2 exposure onto the Si clean surface, no signal was observed at < 100 L, where oxygen pressure of 1×10^{-6} Torr was used. In this oxygen exposure regime of < 100 L, the AE spectrum showed no evidence of SiO_2 growth. These results can be explained in terms of the low oxygen pressure (1×10^{-6} Torr), where the etching is faster than the oxidation at 1050 K [15]. In this study of Si oxidation at > 100 L, we used an oxygen pressure of greater than 7.5×10^{-6} Torr, where Si oxidation is dominant at 1050 K. As clearly shown in the figure, an oxygen exposure of 150 L at 1050 K results in the sudden appearance of the signal. Even after an exposure of 6×10^6 L oxygen molecules, the spin density remains almost constant at $2.5\text{--}3.0 \times 10^{12} \text{ cm}^{-2}$. The good reproducibility of this phenomenon for alternating cycles of oxidation and thermal heating at 1570 K was confirmed. This interface defect density is almost the same as the well-known P_b centers for the case without hydrogenation [2,4].

The thickness of the SiO_2 was approximately 0.25 nm at 10^4 L. The Si-Si bond length in silicon crystal is 0.23 nm, and the Si-O-Si structure in SiO_2 is such that two Si-O bonds each 0.16 nm long make an angle of 141° . Therefore the oxide thickness at 150–1000 L corresponds to oxidation of one or two Si atomic layer(s). In order to

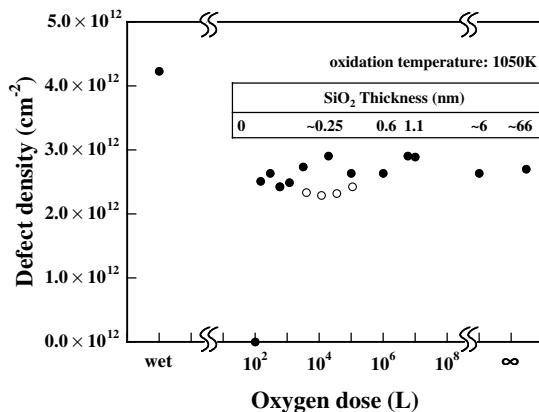


FIG. 3. Defect density estimated from the double integration plotted as a function of oxygen dose. "Wet" indicates the sample after wet (RCA) cleaning. Solid circles, results under various oxygen partial pressures. Open circles, results under a constant oxygen partial pressure (4×10^{-5} Torr). The samples of 6 and 66 nm were oxidized in different ways from UHV oxidation described in the text. In both case, the oxidation temperature is 1050 K.

study the thickness dependence of the interfacial defects over a wider range, the P_b density of further oxidized films of 6 and 66 nm was measured. The former was prepared in the same chamber under an O_2 pressure of 0.5 atm at 1050 K, and the latter was prepared in a different furnace chamber under a pressure of 1 atm at 1170 K after exposure to air. The thickness of these samples was measured using an ellipsometry technique in ambient air at room temperature. As shown in the figure, the interface defect density is similar to that observed in the cases of thinner SiO_2 . These results strongly suggest that the oxidation of one or two Si atomic layer(s) already produces almost the same amount of defect density as that observed at the interface with a thick SiO_2 film.

Interface defects are usually explained in terms of the interface strain between two materials. It is widely known that hetero-epitaxial growth accumulates strain due to lattice mismatch between two materials with increasing thickness of the grown layer until a critical thickness is reached at which structural relaxation occurs by the generation of misfit dislocations at the interface [16]. For example, the critical thickness from 3 to 1000 nm was observed in the $\text{Ge}_x\text{Si}_{1-x}/\text{Si}$ system, where the value of x was varied from 0.7 to 0.1, respectively [17]. On the other hand, it is known that a large strain at the Si/ SiO_2 interface builds up because Si oxidation proceeds with the insertion reaction of an oxygen atom into a Si-Si bond in the substrate. This reaction approximately doubles the volume per Si atom [18]. Kobeda and Irene observed a large compressive strain in a Si/ SiO_2 system [19], and the dependence of interface stress on SiO_2 thickness (10–80 nm) [20]. From the analogy of the $\text{Ge}_x\text{Si}_{1-x}/\text{Si}$ system, a long-range effect of the interface strain was expected to have a large influence on Si/ SiO_2 interface defect density. However, the present study indicates that such a long-range effect does not affect the defect density in a Si/ SiO_2 interface.

The midgap interface state density (D_{it}) measured by the capacitance-voltage characteristics in a metal-oxide-semiconductor structure with the data of stress measurements in a Si/ SiO_2 system was reported by Bjorkman *et al.* [21]. They found that D_{it} density depends not only on the film stress but also on the SiO_2 thickness. Their observation seems to be inconsistent with the present result because it is known that D_{it} has linear relationship with P_b density for many cases [4], although its relationship is still under discussion [13]. This discrepancy could originate from the following cause. The interface defect density of P_b and D_{it} could be easily changed by varying hydrogen contents in the oxidizing gas [2,13]. For actual device fabrications, the interface of Si/ SiO_2 is treated using H_2 annealing, resulting in a lower interface defect density of around $1 \times 10^{10} \text{ cm}^{-2} \text{ eV}^{-1}$. The amount of D_{it} observed by them was around $1 \times 10^{10} \text{ cm}^{-2} \text{ eV}^{-1}$, which is a typical number for the case after hydrogen gas treatment and is much smaller than our result. Therefore, their

result was for a more complicated situation and effect due to interface defect formation and hydrogen passivation, whereas our experimental setup enabled an ideal hydrogen-free process to be conducted in the UHV chamber, namely, pure experimental conditions for Si oxidation.

Stesmans reported on a precise study of oxidation temperature dependence of P_b density with the conditions of as-oxidized and dehydrogenation annealing at 1060 K [2]. He speculated that P_b generation in the temperature range $470 < T < 1320$ K was essentially the result of the intrinsic interface stress of Si/SiO₂ determined at the Si/SiO₂ interface plane by comparing with the oxidation temperature dependence of interface stress reported by Kobeda and Irene [19]. The present result that P_b density is determined by the oxidation of one or two Si atom layer(s) is consistent with his speculation. The oxygen partial pressure and the oxidation time were varied in this study. It is realistic to vary both the oxygen partial pressure and the oxidation time to control the thickness of SiO₂ films, since the oxidation rate changes drastically depending on oxygen pressure and SiO₂ thickness. For example, precise control of a SiO₂ film with 0.25 nm could be achieved under relatively lower pressure (7.5×10^{-6} – 5×10^{-5} Torr). On the contrary, for relatively thicker film (> 1 nm) a higher oxygen pressure ($\approx 8 \times 10^{-3}$ Torr) was used. In the figure, the results of a series of experiments under a constant oxygen partial pressure (4×10^{-5} Torr) are shown with open circles for comparison, whereas the closed circles represent those for various oxygen pressures ranging from 7.5×10^{-6} to 8×10^{-3} Torr. As shown in the figure, the P_b density is almost constant and essentially independent of the oxygen partial pressure, and therefore oxidation rate. As shown in the figure, the P_b density is almost constant for various oxygen pressures. This result suggests that in the present conditions the chemical reaction, including P_b center creation, is fast enough to achieve the energetically favorable structure. The dependencies of the precisely controlled oxygen pressure and the oxidation time in addition to the oxidation temperature will give us more perfect understandings of dynamic Si oxidation processes.

To understand the interface defect formation, a theoretical study of the Si oxidation process will be necessary, although there have been some efforts to clarify the network change due to microscopic chemical reactions in Si oxidation [22]. In this Letter, we showed that defect formation would be completed within oxidation of the initial one or two Si layer(s). This information should provide a basis for theoretical models and assist theoretical studies because a complete understanding of interface defect formation does not require calculations with a thick Si oxidation process but with oxidation of only a couple of Si layers.

In summary, we reported the first observation of the formation process of interface defects (P_b centers) of

Si(111) oxidation at 1050 K. The number of P_b centers of the initial one or two layer(s) Si oxidation almost reached the value of 2.5 – 3.0×10^{12} cm⁻² and was almost independent of SiO₂ thickness. This result indicates that the interface defects of Si/SiO₂ do not originate from the long-range accumulation of structural stress between two materials, but from the chemical reactions of oxidation within the first few layers of Si atoms.

This work was partly supported by NEDO. The authors greatly appreciated helpful discussions with Dr. T. Yasuda (AIST), Dr. M. Nishizawa (AIST), Dr. T. Yamasaki (Fujitsu), Dr. T. Uda (Hitachi), and Dr. K. Kato (Toshiba).

-
- [1] M. Cook and C.T. White, Phys. Rev. B **38**, 9674 (1988).
 - [2] A. Stesmans, Phys. Rev. B **48**, 2418 (1993).
 - [3] A. Stesmans and V.V. Afanas'ev, Phys. Rev. B **57**, 10 030 (1998).
 - [4] E. H. Poindexter, G.J. Geradi, M.-E. Rueckel, P.J. Caplan, N.M. Johnson, and D.K. Biegelsen, J. Appl. Phys. **56**, 2844 (1984).
 - [5] R. Helms and E. H. Poindexter, Rep. Prog. Phys. **57**, 791 (1994).
 - [6] P.M. Lenahan and J.F. Conley, Jr., J. Vac. Sci. Technol. B **16**, 2134 (1998).
 - [7] K.L. Brower, Appl. Phys. Lett. **43**, 1111 (1983).
 - [8] See The International Technology Roadmap for Semiconductors (Semiconductor Industry Association, CA).
 - [9] M.L. Green, E.P. Gusev, R. Degraeve, and E. Garfunkel, J. Appl. Phys. **90**, 2057 (2001).
 - [10] T. Umeda, M. Nishizawa, T. Yasuda, J. Isoya, S. Yamasaki, and K. Tanaka, Phys. Rev. Lett. **86**, 1054 (2001).
 - [11] W. Futako, M. Nishizawa, T. Yasuda, J. Isoya, and S. Yamasaki, J. Vac. Sci. Technol. B **19**, 1898 (2001).
 - [12] W. Kern, RCA Eng. **28**, 99 (1983).
 - [13] E. Cartier, J.H. Stathis, and D.A. Buchman, Appl. Phys. Lett. **63**, 1510 (1993).
 - [14] T. Yasuda, S. Yamasaki, M. Nishizawa, N. Miyata, A. Shklyayev, M. Ichikawa, T. Matsudo, and T. Ohta, Phys. Rev. Lett. **87**, 037403 (2001).
 - [15] B. Mohadjeri, M.R. Baklanov, E. Kondoh, and K. Maex, J. Appl. Phys. **83**, 3614 (1998).
 - [16] J.W. Matthews, S. Mader, and T.B. Light, J. Appl. Phys. **41**, 3800 (1970); J.W. Matthews, in *Dislocations in Solids*, edited by F.R.N. Nabarro (North-Holland, Amsterdam, 1982), Vol. 2, p. 461.
 - [17] R. People and J.C. Bean, Appl. Phys. Lett. **47**, 322 (1985).
 - [18] T.J. Delph, J. Appl. Phys. **83**, 786 (1998).
 - [19] E. Kobeda and E.A. Irene, J. Vac. Sci. Technol. B **4**, 720 (1986).
 - [20] E. Kobeda and E.A. Irene, J. Vac. Sci. Technol. B **6**, 574 (1988).
 - [21] C.H. Bjorkman, J.T. Fitch, and G. Lucovsky, Appl. Phys. Lett. **56**, 1983 (1990).
 - [22] H. Kageshima and K. Shiraishi, Phys. Rev. Lett. **81**, 5936 (1998).